

Cumulative light curves of gamma-ray bursts and relaxation systems

S. McBreen¹, B. McBreen¹, L. Hanlon¹, and F. Quilligan^{1,2}

¹ Department of Experimental Physics, University College Dublin, Dublin 4, Ireland

² Intel Corporation, Leixlip, Co. Kildare, Ireland

Received / Accepted

Abstract. The cumulative light curves of a large sample of gamma ray bursts (GRBs) were obtained by summing the BATSE counts. The smoothed profiles are much simpler than the complex and erratic running light curves that are normally used. For most GRBs the slope of the cumulative light curve (S) is approximately constant over a large fraction of the burst. The bursts are modelled as relaxation systems that continuously accumulate energy in the reservoir and discontinuously release it. The slope is a measure of the cumulative power output of the central engine. A plot of S versus peak flux in 64 ms ($P_{64\text{ms}}$) shows a very good correlation over a wide range for both long and short GRBs. No relationship was found between S and the GRBs with known redshift. The standard slope (S'), which is representative of the power output per unit time, is correlated separately with $P_{64\text{ms}}$ for both sub-classes indicating more powerful outbursts for the short GRBs. S' is also anticorrelated with GRB duration. These results imply that GRBs are powered by accretion into a black hole.

Key words. Gamma rays – bursts: Gamma rays – observations: Methods – data analysis: Methods – statistical

1. Introduction

Cosmological gamma ray bursts (GRBs) emit an extraordinary amount of energy in gamma rays (Costa et al., 1997; van Paradijs et al., 1997; Piran, 1999). The source of this energy may be a cataclysmic event involving mergers of compact objects such as neutron star binaries or neutron stars and black hole binaries (Ruffert & Janka, 1999) or the formation of a black hole during or after the collapse of massive stars (Rees & Mészáros, 1994; Paczynski, 1998; Vietri & Stella, 1998; MacFadyen & Woosley, 1999; Reeves et al., 2002). GRB light curves are complex and erratic (Fishman & Meegan, 1995). There are a number of recent results on the properties of the pulses in GRBs and their relationship to the duration T_{90} (Ramirez-Ruiz & Fenimore, 2000; Salmonson, 2000; Norris, 2002; McBreen et al., 2002a; Gupta et al., 2002; Quilligan et al., 2002 and references therein). The correlated pulses in GRBs have a unique set of properties. In this paper we show in sections 3 and 4 that the slope of the cumulative light curve of most short and long GRBs is approximately linear and the bursts can be modelled as relaxation systems. In addition the slopes are highly correlated with the peak flux and anticorrelated with GRB duration. The large and uniform BATSE sample of GRBs were used in this analysis (Fishman & Meegan, 1995; Kouveliotou et al., 1993).

2. Timing analysis of the GRB profiles

A large sample of 498 of the brightest BATSE GRBs with data combined from the four energy channels was analysed and denoised using either wavelets or median filters. A detailed account of this process including sample selection and pulse analysis in GRBs has been given elsewhere (Quilligan et al., 2002; McBreen et al., 2001). The GRB sample was restricted here to bursts that had the on-board summed count from only two Large Area Detectors and includes 55 GRBs with $T_{90} < 2$ s analysed at 5 ms resolution, 250 GRBs with $T_{90} > 2$ s at 64 ms resolution. To extend the sample to include additional GRBs with $T_{90} > 100$ s, a further 71 GRBs were included and analysed at 256 ms resolution. The cumulative light curve was obtained by converting the BATSE rates to counts and taking the cumulative sum. The cumulative count from the same number of on-board detectors is uncorrected for the detector response and the angles between the detectors and GRB sources. The errors from these effects should be less than $\pm 30\%$. As a check on this procedure, the cumulative count for the GRBs was compared with the BATSE fluences. There is a high degree of correlation between the two quantities showing that the cumulative count from the same number of detectors is a good measure of the burst. There is close agreement with the cumulative light curves obtained in the spectroscopic sample of Preece et al. (2000).

3. Results

The running and cumulative light curves of a sample of bursts, that cover a wide range in T_{90} , are given in Fig. 1. The cumulative light curves smooth the running profiles. The slope of the cumulative light curve (S) was measured for the section of the GRB that included more than 50% of the total counts and could be represented by a straight line, with a precision in the measured slope that was always much better than a factor of 2. Not all GRBs were fit with a single straight line because of long time intervals with very little or no emission (Fig. 1d) and some of these GRBs have been discussed by Ramirez-Ruiz & Merloni (2001). In these cases two or more straight lines were used to fit the separate periods of emission. The average value of the slopes was adopted for that GRB. This procedure was used for 66 GRBs with $T_{90} > 2$ s and 2 GRBs with $T_{90} < 2$ s. The cumulative light curves of a number of GRBs have measurable curvature and in these cases a curve is a more accurate fit than the straight line adopted here. These GRBs are the subject of a separate publication (McBreen et al., 2002b).

The median percentage of the integrated counts over which the slope was measured is 71% for GRBs with $T_{90} > 2$ s and 83% for short GRBs. The corresponding values of the median percentages of T_{90}/T_{50} are 34%/127% and 68%/140%. T_{50} is a better measure than T_{90} of the active period of the burst over which the slopes were measured. It is also better anticorrelated with the slope than T_{90} (Table 1, Fig. 2c). This effect is illustrated in Fig. 1d where 75% of the integrated counts is used for the slope over only 24% of T_{90} whereas in Fig. 1a the corresponding values are 69% and 59% respectively. There is a long quiescent interval in the GRB in Fig. 1d which contributes to the small percentage value of T_{90} .

The slopes of the cumulative light curves of 376 GRBs are plotted in Fig. 2a versus the peak flux in 64 ms ($P_{64\text{ms}}$). There is a good correlation between S and $P_{64\text{ms}}$. Spearman rank order correlation coefficients ρ , associated probabilities and index of best fit power law for these quantities are listed in Table 1. The standard slope S' was obtained by dividing the slope of the cumulative counts (S) by the time over which the slope was measured and hence it represents the cumulative counts or power output of the source per unit time. The standard slope is plotted versus $P_{64\text{ms}}$ in Fig. 2b. The correlation coefficients are listed in Table 1 for short and long GRBs. The best fit power laws have indices close to 1.6 for both classes of GRBs but there is considerable spread in the values with the short bursts displaced from the long bursts by $\sim 10^2$.

The standard slope is plotted versus T_{50} in Fig. 2c. The correlation coefficient is -0.90 with a best fit power law index of -1.1. The corresponding values for T_{90} are -0.85 and -1.08 respectively. The values are also listed in Table 1 for T_{90} and T_{50} versus S. S' is better anticorrelated with duration than S.

Fenimore (1999) obtained the average temporal profile of 98 GRBs by normalising to a standard duration

Table 1. Spearman rank order correlation coefficients, ρ , the associated probabilities and index of the best fit power law for a range of GRB properties. In all cases the high values of ρ show either strong correlations or anticorrelations between the burst properties.

Properties	ρ	Probability	Power Law Index
$P_{64\text{ms}}$ vs. S	0.84	$< 10^{-48}$	1.04
$P_{64\text{ms}}$ vs. S' ($T_{90} > 2$ s)	0.72	$< 10^{-48}$	1.63
$P_{64\text{ms}}$ vs. S' ($T_{90} < 2$ s)	0.69	6.1×10^{-9}	1.65
T_{90} vs. S'	-0.85	$< 10^{-48}$	-1.08
T_{90} vs. S ($T_{90} > 2$ s)	-0.58	1.7×10^{-30}	-0.54
T_{90} vs. S ($T_{90} < 2$ s)	-0.39	3.0×10^{-3}	-0.37
T_{50} vs. S'	-0.9	$< 10^{-48}$	-1.10
T_{50} vs. S ($T_{90} > 2$ s)	-0.64	1.9×10^{-31}	-0.53
T_{50} vs. S ($T_{90} < 2$ s)	-0.53	3.7×10^{-5}	-0.32
Fluence vs. Cumulative counts	0.92	$< 10^{-48}$	0.92

and a standard peak counts. The average profile is reasonably flat over more than 50% of the duration (Fig. 1b in Fenimore (1999)) implying a linear increase in the cumulative profile and hence in agreement with the results presented here.

4. Discussion

4.1. GRBs as relaxation systems

It can be assumed that the sum of the counts in the bursts (Fig. 1.) is a good measure of the integrated energy emitted by the source because the peak energy lies well within the BATSE band (Fishman & Meegan, 1995). Many models of GRBs consist of a newly formed black hole that accretes from a remnant torus that is cooled by neutrino emission (Popham et al., 1999; Narayan et al., 2001; Lee & Ramirez-Ruiz, 2002). The energy to drive the relativistic jets and bursts may be extracted from the disk and spinning black hole by MHD processes and neutrino annihilation. The efficiency of these processes in creating relativistic jets is on the order of one percent (MacFadyen & Woosley, 1999)

Models of this type can be usefully compared with a relaxation system (Palmer, 1999) which is taken to be one that continuously accumulates energy from the accretion process and discontinuously releases it. The energy in the reservoir at any time t is

$$E(t) = E_o + \int_o^t R(t)dt - \Sigma S_i \quad (1)$$

where E_o is the energy stored in the reservoir that accumulates energy at a rate $R(t)$ and discontinuously releases events of size S_i .

The simplest system is referred to as a relaxation oscillator where there is a fixed level or trip-point that triggers a release of the energy when $E = E_{\text{max}}$. The soft gamma ray repeater (SGR) (Palmer, 1999; Göğüs et al.,

2000; Hurley et al., 1994) and GRB pulses are not consistent with this oscillator. More complicated behaviour occurs when the accumulation rate, trigger rate or release strength are not constant. If the system starts from a minimum level $E = E_{\min}$, accumulates energy at a constant rate $R = r$, the sum of the releases is approximately a linear function of time i.e. $\Sigma S_i \propto rt$. This model can account for the approximately linear increase in cumulative counts from GRBs (Fig 1). The pulses in GRBs have a tendency to keep the cumulative count close to a linear function and maintain a steady state situation.

Ramirez-Ruiz & Merloni (2001) found a correlation between the duration of an emission episode in a multi-peaked burst and the duration of the preceding quiescent time which is similar to the above scenario. The system could build up its energy probably via an MHD instability driven dynamo and reach a near critical or metastable level. A local instability could cause a rapid dissipation of all the stored energy. The system will tend to return to a more stable configuration characterised by a certain threshold energy E_o , or a sub-critical magnetic field configuration. The source then becomes quiescent. Interestingly both models can be unified by noting that each time the system is completely drained by a total release of accumulated energy, the central engine goes quiescent but otherwise the energy extraction is usually in episodes that are incomplete releases of energy. In this case the longer the quiescent time, the higher the stored energy from the next episode. Such a situation may give rise to the observed correlations between long quiescent times (Ramirez-Ruiz & Merloni, 2001), correlated pulse properties and intervals between pulses (Quilligan et al., 2002; McBreen et al., 2002a; Nakar & Piran, 2002). This is a different mechanism from any relaxation oscillator which forces a release of energy when the system reaches an upper level.

4.2. Relationships between the slopes and peak flux

There is a significant correlation, that extends over a range of $\sim 10^3$, between $P_{64\text{ms}}$ and S (Fig. 2a and Table 1). The seven GRBs, detected by BATSE, with measured redshifts are also plotted in Fig. 2. These sources cover a wide range with no obvious relationship between S , $P_{64\text{ms}}$ and z .

The separation of GRBs into two sub-classes was characterised by durations > 2 s and < 2 s (Kouveliotou et al., 1993). The plot of the standard slope versus $P_{64\text{ms}}$ (Fig. 2b) also separates the GRBs into two classes with the short GRBs having a more powerful output power per unit time. The cosmological GRBs with known redshift have values of S and S' that range from 7×10^{44} to 5×10^{47} Watts and 1.5×10^{44} to 2×10^{46} Watts per second respectively. There is no evidence for a new class of GRBs with a different relationship between the standard slope and $P_{64\text{ms}}$.

4.3. Relationships between the slopes and durations

The data presented in Fig. 2c shows that as the standard slope increases the values of T_{50} decrease and this effect is present in both sub-classes (Table 1). The trend is quite revealing and shows that the smaller the value of T_{50} the greater the standard slope or the cumulative power output per second from the source. The standard slope plays an important role in determining T_{50} . The median values of the pulse properties and time intervals between pulses were found to increase with T_{90} (McBreen et al., 2002a). The opposite relationship exists here between S' and burst duration (Table 1) implying that as the standard slope increases there is a corresponding decrease in the pulse properties. GRBs with high accretion rates have large values of the standard slope, fast pulses and short durations whereas lower accretion gives lower values of S' , slower pulses that are further apart and larger values of T_{90}/T_{50} . These results provide strong evidence that GRBs are powered by hyperaccretion into a black hole from a standard type engine (Salmonson, 2000; Frail et al., 2001; Panaitescu & Kumar, 2001; Piran et al., 2001).

References

- Castro-Tirado, A. J. 2001, [astro-ph/0102122]
 Costa, E., Frontera, F., Heise, J. et al. 1997, Nature, 387, 783
 Fenimore, E. E. 1999, ApJ, 518, 375
 Fishman, G. J. & Meegan, C. A. 1995, Ann. Rev. Astron. Ap., 33, 415
 Frail, D. A., Kulkarni, S. R., Sari, R., et al. 2001, ApJ, 562, L55
 Göğüs, E., Woods, P. M., Kouveliotou, C. et al. 2000, ApJ, 532, L121
 Gupta, V., Das Gupta, P. & Bhat, P. 2002, [astro-ph/0206402]
 Hurley, K. J., McBreen, B., Rabbette, M., & Steel, S. 1994, A&A, 288, L49
 Kouveliotou, C., Meegan, C. A., Fishman, G. J., et al. 1993, ApJ, 413, L101
 Lee, W. H. & Ramirez-Ruiz, E. 2002, [astro-ph/0206011]
 MacFadyen, A. I. & Woosley, S. E. 1999, ApJ, 524, 262
 McBreen, S., McBreen, B., Quilligan, F., & Hanlon, L. 2002a, A&A, 385, L19
 McBreen, S., McBreen, B., Hanlon, L., & Quilligan, F. 2002b, (A&AL in press)
 McBreen, S., Quilligan, F., McBreen, B., Hanlon, L. & Watson, D. 2001, A&A, 380, L31
 Narayan, R., Piran, T. & Kumar, P. 2001, ApJ, 557, 949
 Nakar, E. & Piran, T. 2002, ApJ, 572, L139
 Norris, J. P. 2002, [astro-ph/0201503]
 Paczynski, B. 1998, ApJ, 494, L45
 Panaitescu, A. & Kumar, P. 2001, ApJ, 560, L49
 Palmer, D. M. 1999, ApJ, 512, L113
 Piran, T. 1999, Phys. Report, 314, 575
 Piran, T. Kumar, P. Panaitescu, A. & Piro, L. 2001, ApJ, 560, L167
 Popham, R., Woosley, S. E. & Fryer, C. 1999, ApJ, 518, 356
 Preece, R. D., Briggs, M. S., Malozzi, R. S. et al. 2000, ApJS, 126, 19
 Quilligan, F., McBreen, B., Hanlon, L. et al. 2002, A&A, 385, 377

- Ramirez-Ruiz, E. & Fenimore, E. E. 2000, ApJ, 539, 712
 Ramirez-Ruiz, E. & Merloni, A. 2001, MNRAS, 320, L25
 Rees, M. J. & Mészáros, P. 1994, ApJ, 430, L93
 Reeves, J. N., Watson, D., Osborne, J. P. et al. 2002, Nature, 416, 512
 Ruffert, M. & Janka, H. T. 1999, A&A, 344, 573
 Salmonson, J. D. 2000, ApJ, 544, L115
 van Paradijs, J., Groot, P. J., Galama, T. et al. 1997, Nature, 386, 686
 van Paradijs, J., Kouveliotou, C. & Wijers, R. A. M. J. 2000, Ann. Rev. Astron. Ap., 38, 379
 Vietri, M. & Stella, L. 1998, ApJ, 507, L45

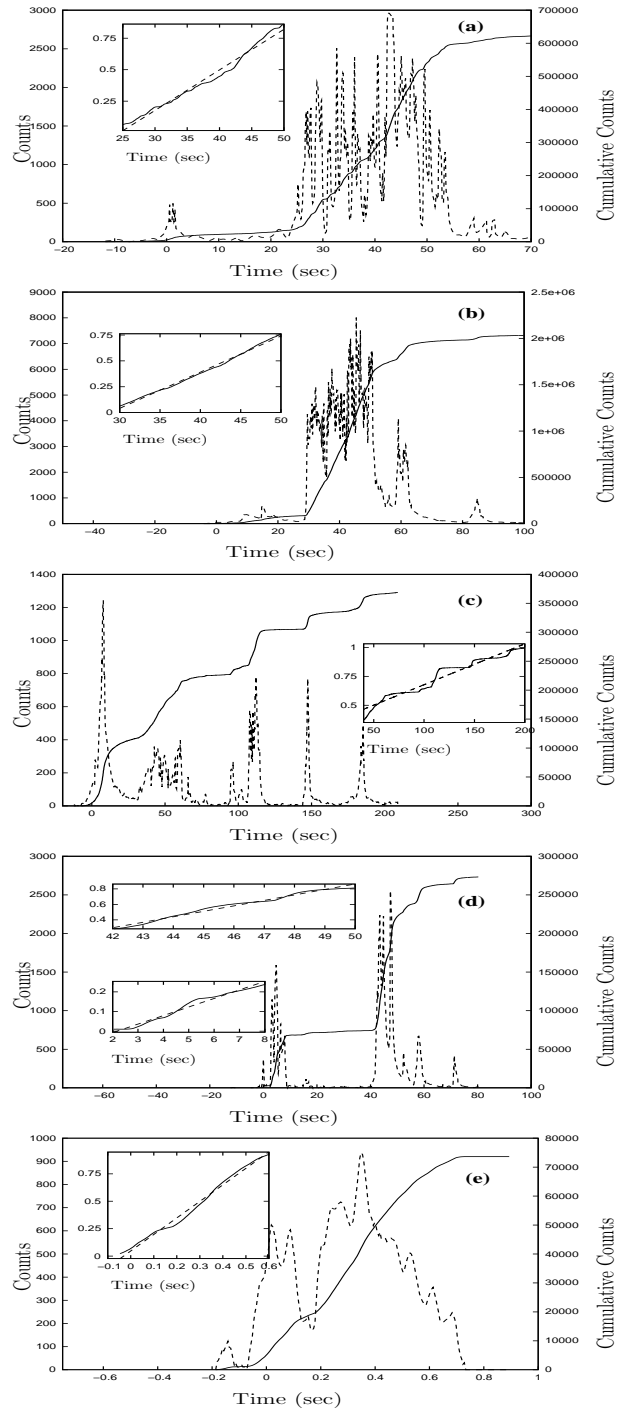


Fig. 1. The running (dashed) and cumulative (solid) light curves of the BATSE bursts with trigger numbers a) 3128, b) 3057, c) 3042, d) 7560, e) 2217 with count per 64 ms and cumulative count scales on the left and right vertical axes. The insert gives the straight line fit (dashed) to the cumulative count (solid) for the relevant section(s) of the GRB. The vertical axes in the inserts are the normalised cumulative count.

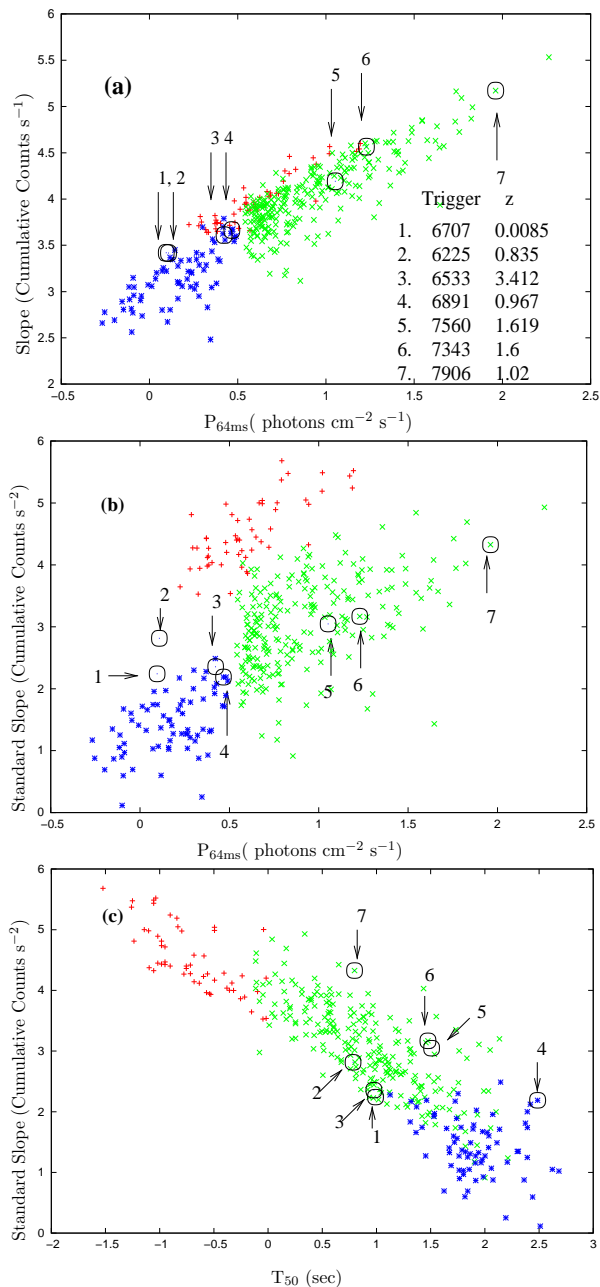


Fig. 2. The values of P_{64ms} are plotted versus a) the slope S and b) the standard slope S' of the GRB cumulative light curve for three categories of GRBs i.e. $T_{90} < 2$ s (red), $T_{90} > 2$ s (green) and the additional sample with $T_{90} > 100$ s (blue). T_{50} is plotted versus S' in c) for the same three categories. The seven GRBs with known redshift and detected by BATSE are labelled (van Paradijs et al., 2000; Castro-Tirado, 2001 and references therein). The BATSE trigger numbers and redshifts are given in the top figure. An extension of the peak flux limited sample with $T_{90} > 2$ s to lower values should populate the region containing GRBs 1 and 2 with known z in b).